

# Application of CSA - BP Neural Network in Gearbox Fault Diagnosis

Lijun Wang, Shengfei Ji and Nanyang Ji

**Abstract**—Cuckoo Search Algorithm as a new group intelligent optimization algorithm is developed in recent years. In this paper, the algorithm of cuckoo search optimization BP neural network is applied to the gearbox fault diagnosis for the first time. The operating states of the gearbox include normal operation, gear missing teeth, tooth surface wear and gear eccentricity. Meanwhile, in order to reduce the interference of noise on the fault identification, the collected vibration signal is denoised by using the decomposition and reconstruction to wavelet packet. The parameters of BP neural network are optimized by the Cuckoo Search Algorithm and used to determine the gearbox fault identification. Finally, the recognition results are compared with the results of GA - BP neural network and PSO - BP neural network. The results show that this algorithm can identify the status of each condition and achieve diagnostic recognition in gearbox fault diagnosis. Therefore, it not only plays a key role in reducing property damage and personal injury caused by equipment damage, but also has very important significance for its research in other fault areas.

**Keywords**—CSA - BP neural network, wavelet packet denoising, fault diagnosis

## I. INTRODUCTION

In 2009, Yang and Deb proposed a new heuristic called the Cuckoo Search Algorithm (CSA)<sup>[1]</sup>. The algorithm is the introduction of some birds' Levi flight mechanism, which mimics cuckoo spawning activities. CSA has the advantages of simple structure and less control parameters and it is widely used in project scheduling<sup>[2]</sup>, engineering optimization<sup>[3]</sup> and solving displacement scheduling problems<sup>[4]</sup>. According to the characteristics and application fields of CSA, the algorithm is applied to the fault diagnosis of gearbox for the first time.

In CSA, let  $x_i^t = (x_{i1}^t, x_{i2}^t, \dots, x_{in}^t)^T$  denote the location of the  $i$ -th nest in the  $t$ -th dimension in the  $n$ -dimensional optimization

This work was supported by Plan for Scientific Innovation Talent of Henan Province (164100510018), Plan for Scientific Innovation Talent of Henan Province (154200510020), Postgraduate Education Reform Project of Henan Province (2017SJGLX006Y), Zhengzhou Measuring & Control Technology and Instrumentations Key Laboratory (121PYFZX181), Innovation Scientists and Technicians Troop Construction Projects of Henan Province (2011-39) and the Ninth Graduate Student Innovation Project of NCWU(YK-2017-08).

Lijun Wang is with the School of Mechanical Engineering, North China University of Water Resources and Electric Power, Zhengzhou 450045, Henan, China (corresponding author; e-mail: wljmb@163.com).

Shengfei Ji is with the the School of Mechanical Engineering, North China University of Water Resources and Electric Power, Zhengzhou 450045, Henan, China.

Nanyang Ji is with the the School of Mechanical Engineering, North China University of Water Resources and Electric Power, Zhengzhou 450045, Henan, China.

problem. The new nest location is updated by the following formula:

$$x_i^{(t+1)} = x_i^t + \alpha \oplus L(\lambda). \quad (1)$$

Where,  $x_i^{(t+1)}$  represents the location of the nest,  $\alpha$  represents the step size factor,  $\oplus$  symbol represents the point-to-point multiplication.  $L(\lambda)$  represents a random search vector produced by the Levi distribution obeying parameter  $\lambda$ , that is:

$$L(\lambda) = 0.01 \frac{u}{|v|} (x_i^{(t)} - x_b^{(t)}). \quad (2)$$

Where,  $u = t^{-\lambda}$ ,  $1 < \lambda < 3$ .  $u$  and  $v$  obey the normal distribution, that is:  $u \sim N(0, \sigma_u^2)$ ,  $v \sim N(0, 1)$ ,

$$\sigma_u = \left[ \frac{\Gamma(\lambda) \sin(0.5\pi(\lambda-1))}{2^{(\lambda-2)/2} \Gamma(0.5\lambda)(\lambda-1)} \right]^{1/(\lambda-1)}.$$

$x_b^{(t)}$  represents the optimal nest position stored at time  $t$ , and  $\Gamma$  is a standard Gamma function. The variance and mean of the probability distribution are unbounded.

CSA specific operation is as follows:

- (1) Produce a certain number of bird nests and spawn in a certain space, and store the best bird's nest at present.
- (2) Update the nest position and spawn by using the formula of step size.
- (3) If the host discovers cuckoo's eggs, abandon the nest and establish a new nest or accept the updated bird nest.
- (4) Calculate the entire nest every iteration and choose the best nest storage.
- (5) Repeat the above process until the cuckoo finds the best nest location.

## II. BP NEURAL NETWORK ALGORITHM MODEL

As shown in Fig.1, it is a structural model of the BP neural network<sup>[5]</sup>. The number of fault types used to test gear generation is  $m$ , that is, the number of input nodes in BP neural network is  $m$ , the number of hidden layer nodes is  $q$ , the number of output nodes is  $l$  and the mapping is constructed by  $f: R^m \rightarrow R$ .

The input of hidden nodes is:

$$S_j = \sum_{i=1}^n \omega_{ij} x(i) - \theta_j \quad (3)$$

Where,  $\omega_{ij}$  is the connection weight from the input layer to the hidden layer,  $\theta_j$  is the threshold of the hidden layer node.

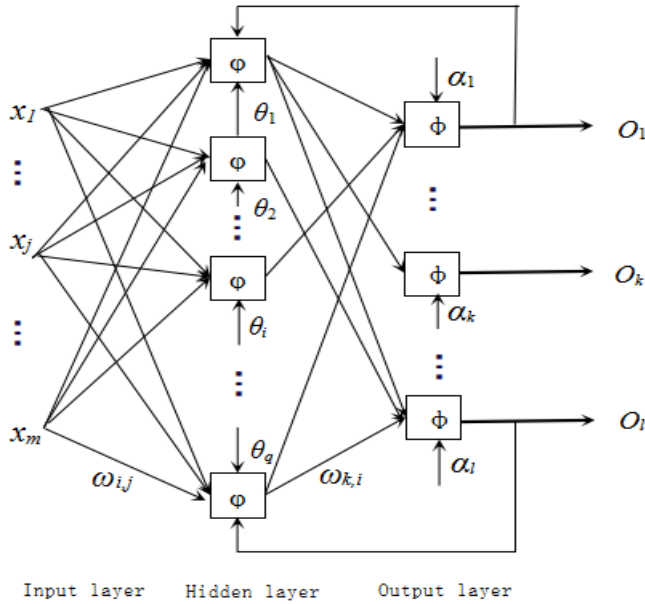


Fig. 1. BP neural network structure model

The output of hidden nodes is:

$$b_j = \frac{l}{1 + \exp(\sum_{i=1}^n w_{ij} x_i - \theta_j)} \quad (4)$$

The output layer node's input is:

$$L = \sum_{i=1}^p \omega_{ki} b_i - \theta_k \quad (5)$$

The output of the output layer node is:

$$x_{i+1} = \frac{1}{1 + \exp(\sum_{j=1}^l \alpha_j b_j - \gamma)} \quad (6)$$

Where,  $\alpha_j$  represents the connection weight from the hidden layer to the output layer and  $\gamma$  represents the threshold of the output layer.

### III. CSA - BP NEURAL NETWORK ALGORITHM MODEL

BP neural network algorithm is a mature algorithm model. It mainly uses the steepest descent method and gradient descent method to constantly modify the weights and thresholds to

achieve the minimum error. The algorithm has the advantages of simple structure, easy to implement, small amount of computation and strong parallelism. But it also has the disadvantages of low training efficiency, easy to fall into local optimum, and slow convergence speed<sup>[6]</sup>. Therefore, the CSA algorithm can be used to optimize the parameters of BP neural network to solve the problems of low learning efficiency and easy falling into local optimum in BP neural network.

CSA optimizes BP neural network steps are as follows<sup>[7]</sup>:

(1) Initialize the nest number  $n$ ,  $P_a$  and the maximum number of iterations  $N_{max}$  and other parameters.

(2) Randomly generate the initial position of a bird's nest:  $x_i^0 = (x_{i1}^0, x_{i2}^0, \dots, x_{in}^0)^T$ . This corresponds to the initial threshold and connection weight of BP neural network. BP neural network is trained according to the optimized parameter training set and the result is predicted.

(3) According to the prediction result, find out the best bird's nest position  $x_d^0$  and update the nest's position according to formula (1) to get the new nest's position.

(4) Calculate the new nest position, and use the good nest position to replace the poor nest position of the previous generation to obtain a better nest position  $e_k = (x_{i1}^k, x_{i2}^k, \dots, x_{in}^k)^T$ .

(5) Compare  $r$  with  $P_a$ , keep the nest with smaller  $P_a$  in  $e_k$  and update the position of the bigger  $P_a$  nest to get a new set of nest positions, And use a good alternative the poor nest location in  $e_k$  to get a better nest position  $q_k = (x_{i1}^k, x_{i2}^k, \dots, x_{in}^k)^T$ .

(6) Find the best bird nest  $x_d^{(k)}$  in  $q_k$ . If the maximum number of iterations is reached, stop the search and output the best position  $x_d^{(k)}$ . Otherwise, go back to step (3) and continue to optimize.

(7) The parameters corresponding to the optimal bird nest position  $x_d^{(k)}$  are taken as the initial thresholds and weights of BP neural network. The training set is trained to establish a gear box fault diagnosis model.

## IV. CSA - BP NEURAL NETWORK ALGORITHM FOR GEARBOX FAULT DIAGNOSIS

### 1. Laboratory equipment

Fig.2 shows the gear box power simulation system equipment. The gear box power simulation system equipment includes: motor, variable frequency controller, gear box, brake and other parts. The gearbox power simulation system has stable performance, can withstand a certain load impact, and has sufficient space to facilitate the replacement and installation of gears and the installation of monitoring devices. It can simulate many different types of fault conditions and can be applied to the dynamics of gearboxes. Analysis, noise analysis, vibration analysis, health monitoring and fault diagnosis.

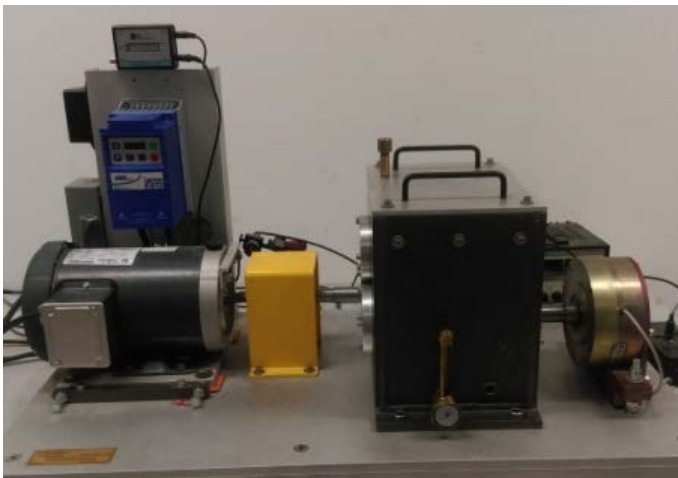


**Fig.2.** Gear box power simulation system equipment

## 2. Signal acquisition

According to the above-mentioned gear box power simulation system equipment, simulate the operating state of the gear box under various working conditions, which are the normal state, gear missing teeth, tooth surface wear, gear eccentricity under the four operating conditions, and under the collection of various working conditions experimental data.

The acquisition signal sensors are set up as shown in Fig. 3. #1-#6 are piezoelectric sensors, which are mainly used to measure the vibration signal under various working conditions. #7 is an acceleration sensor, which is mainly used to measure the rotation speed of the gear shaft.

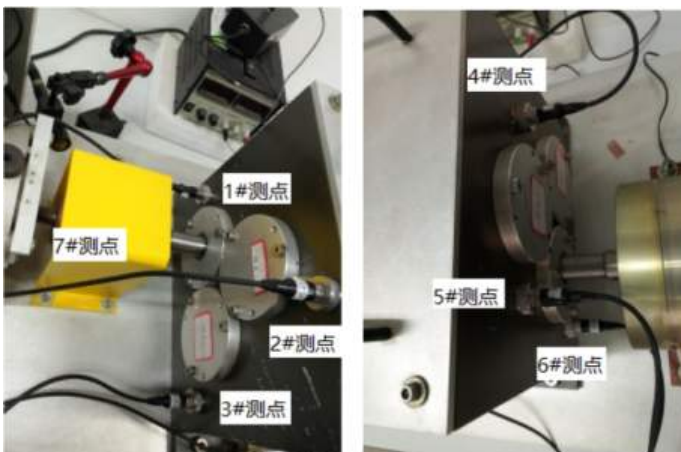


**Fig. 3.** Sensors setting

The data collected for each condition is 100 groups. The former 90 groups data is as training data and the latter 10 groups is as testing data. The collection frequency of each condition is 2000Hz and the collection point is 1024 points. The vibration signals of the collected signal are shown in Fig.4-7.

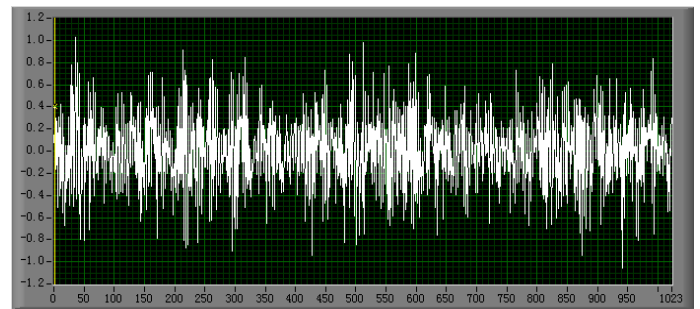


**Fig. 4.** Vibration signal during normal operation

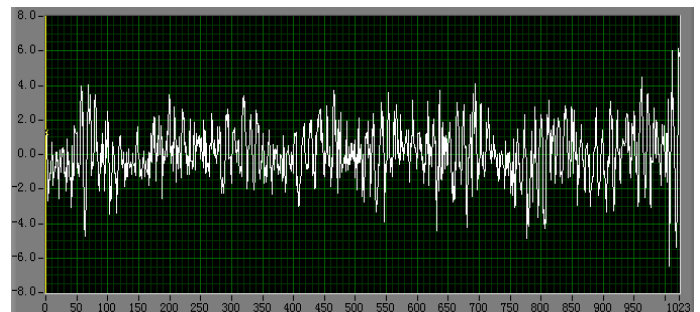


**Fig. 5.** Gear teeth missing tooth vibration signal

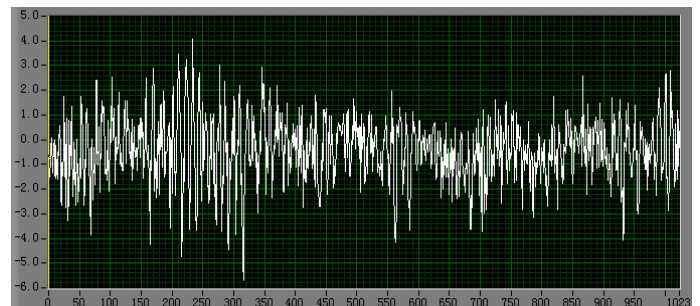


**Fig. 6.** Tooth surface wear vibration signal

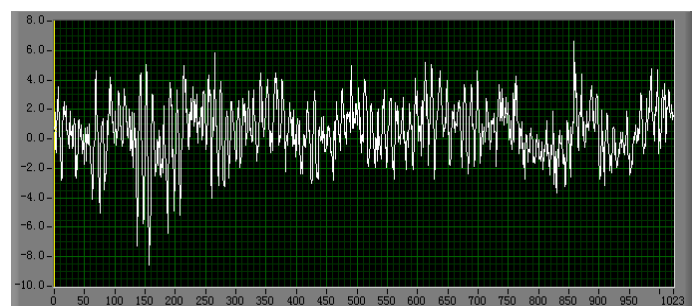


**Fig. 7.** Eccentric gear vibration signal

## 3. Signal denoising

### (1) Wavelet packet principle

From the multi-resolution analysis of square integral real space  $L^2(R)$ , the wavelet approximation space expression is given as<sup>[8]</sup>:

$$L^2(R) = \dots \oplus W_{-1} \oplus W_0 \oplus W_1 \oplus \dots = \bigoplus W_j, \forall j \in Z. \quad (7)$$

Where,  $W_j$  is the wavelet function space;  $j$  is the scale factor;  $\oplus$  is the "orthogonal sum" of the two sub-spaces. Equation (1) shows that Hilbert space  $L^2(R)$  is decomposed into orthogonal sum of wavelet subspace  $W_j (j \in Z)$  according to different scale factor  $j$ . Wavelet packet analysis is further subdivided  $W_j$  by binary mode to achieve the purpose of improving the frequency resolution.

(2) Wavelet packet de-noising process

Wavelet packet de-noising process is as follows<sup>[9]</sup>:

① Wavelet packet decomposition of signal. After selecting a wavelet and determining the desired decomposition level, the signal is wavelet packet decomposed.

② Determine the optimal wavelet packet basis. For a given entropy criterion, compute the optimal tree.

③ Threshold quantization of wavelet packet decomposition coefficients.

④ Signal wavelet packet reconstruction. The noise reduction coefficient is reconstructed by wavelet packet.

Through the wavelet packet decomposition and reconstruction, de-noising processing of the collected signal is finished and the vibration signal decomposition and reconstruction of various conditions are shown in Fig.8-15.

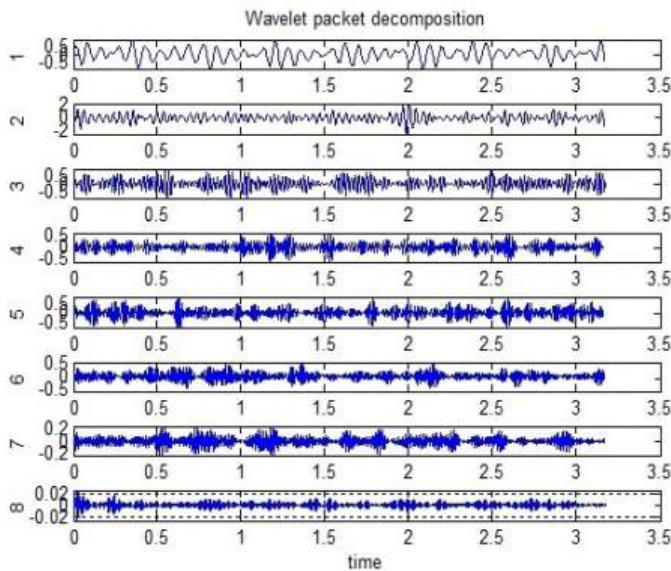


Fig. 8. Wavelet packet decomposition during normal operation

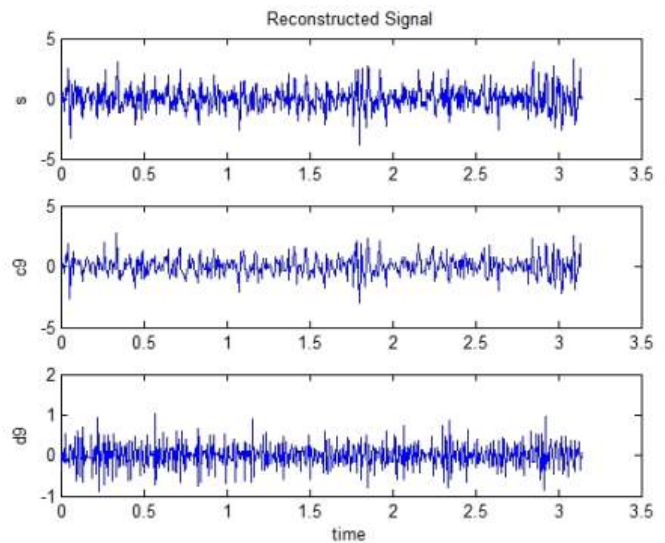


Fig. 9. Wavelet packet reconstruction during normal operation

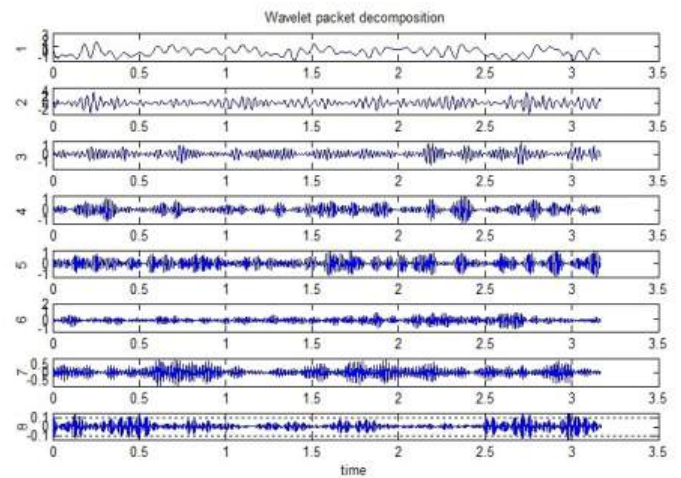


Fig. 10. Wavelet Packet Decomposition with Gear missing tooth

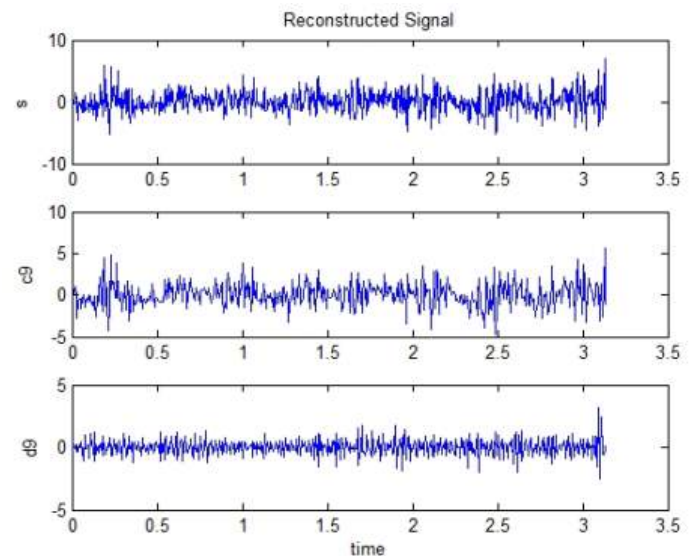


Fig. 11. Wavelet packet reconstruction with Gear missing tooth



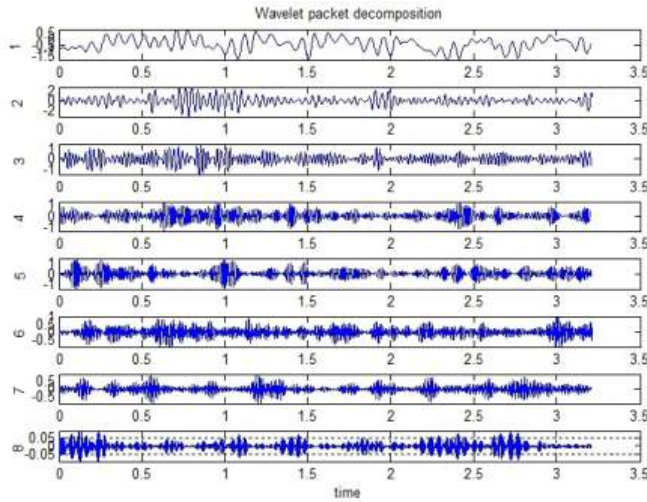


Fig. 12. Wavelet packet decomposition with tooth wear

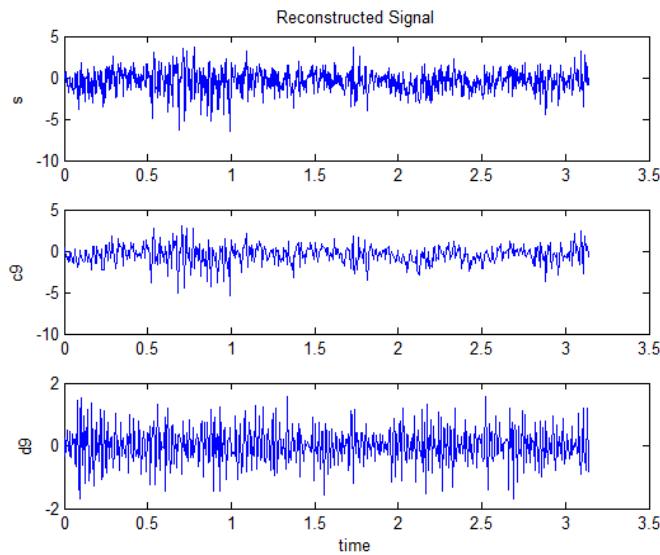


Fig. 13. Wavelet packet reconstruction with tooth wear

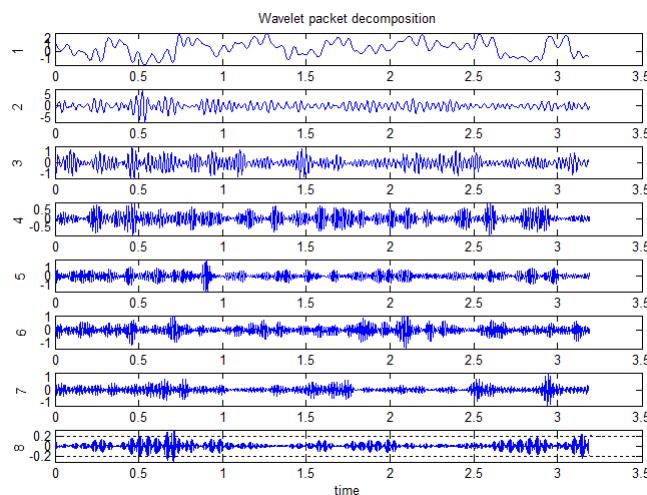


Fig. 14. Wavelet packet decomposition with gear eccentricity

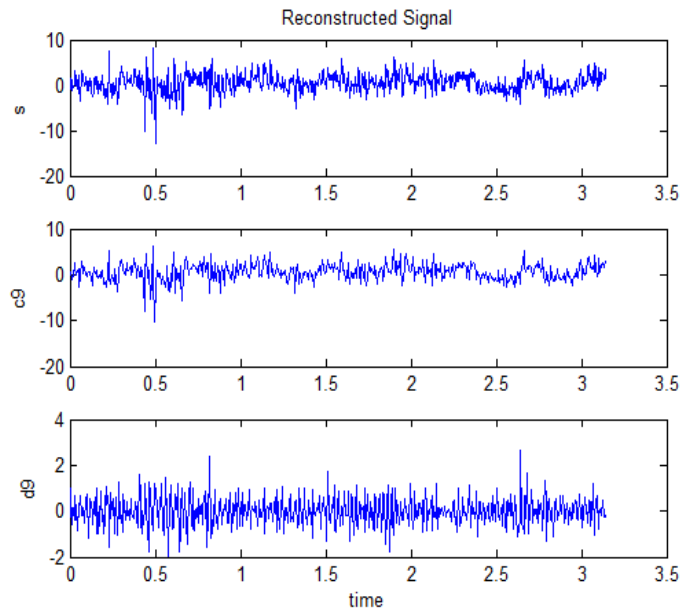


Fig. 15. Wavelet packet reconstruction with gear eccentricity

4. Select the eigenvalue indicator

The eigenvalues of gearbox fault diagnosis are divided into dimension eigenvalue index and dimensionless eigenvalue index. In order to avoid the influence of the dimension on the eigenvalue index, the selected eigenvalues can be used as the basis for the fault diagnosis of the gearbox after the normalization. The normalized formula is <sup>[10]</sup>:

$$x_{ig} = \frac{x_k - x_{\min}}{x_{\max} - x_{\min}} \tag{8}$$

Where,  $x_{ig}$  is the normalized eigenvalue,  $x_k$  is the  $k$ -th eigenvalue and  $x_{\max}$ ,  $x_{\min}$  are respectively the maximum and minimum values of  $x_k$ , respectively.

The characteristic indexes selected in this paper are the eight eigenvalue indexes such as waveform index, peak index and pulse index. The normalized training data and test data are shown in Table 1 and Table 2. Table 1 is part of the gear training data and Table 2 is part of the gear testing data.

**Table. 1.** Part of the gear training data

| Condition                | No. | Waveform indicators | Peak indicators | Pulse indicators | Margin indicators | Skewness indicators | Kurtosis indicators | Square root | Variance indicators | Fault vectors |
|--------------------------|-----|---------------------|-----------------|------------------|-------------------|---------------------|---------------------|-------------|---------------------|---------------|
| Normal working condition | 1   | 0.20414             | 0.71929         | 0.43446          | 0.40062           | 0.43655             | 0.09068             | 0.12765     | 0.02429             | 1 0 0 0       |
|                          | 1   | 0.20932             | 0.83845         | 0.51168          | 0.47414           | 0.44581             | 0.08773             | 0.12141     | 0.02251             | 1 0 0 0       |
|                          | 1   | 0.20350             | 0.59174         | 0.35395          | 0.32389           | 0.44585             | 0.08472             | 0.12112     | 0.02164             | 1 0 0 0       |
|                          | 1   | 0.19335             | 0.66393         | 0.39601          | 0.36200           | 0.43576             | 0.08116             | 0.12588     | 0.02266             | 1 0 0 0       |
| Gear missing tooth       | 1   | 0.21267             | 0.62426         | 0.37733          | 0.34860           | 0.44196             | 0.08308             | 0.11604     | 0.02078             | 1 0 0 0       |
|                          | 2   | 0.45355             | 0.28389         | 0.28463          | 0.28971           | 0.51742             | 0.23144             | 0.05884     | 0.01526             | 0 1 0 0       |
|                          | 2   | 0.51895             | 0.22911         | 0.23661          | 0.24379           | 0.41892             | 0.26754             | 0.04220     | 0.01054             | 0 1 0 0       |
|                          | 2   | 0.69743             | 0.46562         | 0.47931          | 0.48558           | 0.00000             | 0.77986             | 0.04852     | 0.01378             | 0 1 0 0       |
| Tooth wear               | 2   | 0.39731             | 0.57781         | 0.55809          | 0.55515           | 0.49262             | 0.23932             | 0.04966     | 0.01151             | 0 1 0 0       |
|                          | 2   | 0.56601             | 0.45346         | 0.45576          | 0.46500           | 0.58811             | 0.27417             | 0.04232     | 0.01110             | 0 1 0 0       |
|                          | 3   | 0.04986             | 0.21127         | 0.11414          | 0.09987           | 0.03471             | 0.02500             | 0.09098     | 0.01145             | 0 0 1 0       |
|                          | 3   | 0.04689             | 0.15180         | 0.08213          | 0.07108           | 0.01472             | 0.03021             | 0.10106     | 0.01393             | 0 0 1 0       |
| Eccentric gear           | 3   | 0.06542             | 0.21150         | 0.11726          | 0.10418           | 0.00950             | 0.03706             | 0.08462     | 0.01047             | 0 0 1 0       |
|                          | 3   | 0.05245             | 0.19926         | 0.10827          | 0.09413           | 0.01582             | 0.03366             | 0.08758     | 0.01053             | 0 0 1 0       |
|                          | 3   | 0.06450             | 0.16276         | 0.09094          | 0.08132           | 0.00782             | 0.03353             | 0.09867     | 0.01442             | 0 0 1 0       |
|                          | 4   | 0.00000             | 0.18018         | 0.16561          | 0.15668           | 0.05840             | 0.19739             | 0.10201     | 0.03072             | 0 0 0 1       |
| Eccentric gear           | 4   | 0.32685             | 0.17567         | 0.15791          | 0.14925           | 0.45965             | 0.10576             | 0.10281     | 0.03031             | 0 0 0 1       |
|                          | 4   | 0.26853             | 0.15344         | 0.13474          | 0.12499           | 0.40006             | 0.08815             | 0.10239     | 0.02906             | 0 0 0 1       |
|                          | 4   | 0.29708             | 0.13896         | 0.12343          | 0.11438           | 0.47020             | 0.10483             | 0.10395     | 0.03004             | 0 0 0 1       |
|                          | 4   | 0.35298             | 0.16766         | 0.15223          | 0.14551           | 0.61792             | 0.11675             | 0.09442     | 0.02778             | 0 0 0 1       |

**Table. 2.** Part of the gear testing data

| Condition                | No. | Waveform indicators | Peak indicators | Pulse indicators | Margin indicators | Skewness indicators | Kurtosis indicators | Square root | Variance indicators | Fault vectors |
|--------------------------|-----|---------------------|-----------------|------------------|-------------------|---------------------|---------------------|-------------|---------------------|---------------|
| Normal working condition | 1   | 0.25453             | 0.82523         | 0.52178          | 0.49150           | 0.46153             | 0.12463             | 0.49167     | 0.31451             | 1 0 0 0       |
|                          | 1   | 0.20252             | 0.58864         | 0.35170          | 0.32244           | 0.45802             | 0.07862             | 0.48469     | 0.27173             | 1 0 0 0       |
|                          | 1   | 0.17954             | 0.64912         | 0.38225          | 0.34811           | 0.45524             | 0.06887             | 0.47864     | 0.25276             | 1 0 0 0       |
|                          | 1   | 0.16713             | 0.55468         | 0.32033          | 0.28923           | 0.46056             | 0.05471             | 0.48385     | 0.25026             | 1 0 0 0       |
| Gear missing tooth       | 1   | 0.18192             | 0.57589         | 0.33765          | 0.30598           | 0.46567             | 0.06924             | 0.51687     | 0.29056             | 1 0 0 0       |
|                          | 2   | 0.39792             | 0.33132         | 0.32559          | 0.32914           | 0.70308             | 0.17210             | 0.32871     | 0.17088             | 0 1 0 0       |
|                          | 2   | 0.29034             | 0.21358         | 0.20807          | 0.20720           | 0.57144             | 0.16011             | 0.37621     | 0.20067             | 0 1 0 0       |
|                          | 2   | 0.27751             | 0.18777         | 0.18335          | 0.18546           | 0.61894             | 0.09908             | 0.37049     | 0.19743             | 0 1 0 0       |
| Tooth wear               | 2   | 0.37714             | 0.30074         | 0.29527          | 0.29789           | 0.65398             | 0.16022             | 0.39964     | 0.23186             | 0 1 0 0       |
|                          | 2   | 0.46577             | 0.23560         | 0.23949          | 0.24589           | 0.73562             | 0.19058             | 0.32876     | 0.17566             | 0 1 0 0       |
|                          | 3   | 0.05430             | 0.18667         | 0.10192          | 0.08998           | 0.05038             | 0.02560             | 0.35393     | 0.15503             | 0 0 1 0       |
|                          | 3   | 0.03327             | 0.13681         | 0.07204          | 0.06242           | 0.04424             | 0.01576             | 0.35694     | 0.14906             | 0 0 1 0       |
| Eccentric gear           | 3   | 0.04633             | 0.24148         | 0.12943          | 0.11311           | 0.04236             | 0.03033             | 0.35041     | 0.14860             | 0 0 1 0       |
|                          | 3   | 0.07404             | 0.27003         | 0.15059          | 0.13410           | 0.04076             | 0.04180             | 0.33955     | 0.15046             | 0 0 1 0       |
|                          | 3   | 0.04596             | 0.30928         | 0.16516          | 0.14359           | 0.04400             | 0.03106             | 0.34604     | 0.14421             | 0 0 1 0       |
|                          | 4   | 0.35298             | 0.41202         | 0.37168          | 0.35741           | 0.67766             | 0.11751             | 0.46015     | 0.27522             | 0 0 0 1       |
| Eccentric gear           | 4   | 0.27278             | 0.21101         | 0.18613          | 0.17479           | 0.49517             | 0.08827             | 0.46023     | 0.26560             | 0 0 0 1       |
|                          | 4   | 0.23755             | 0.11710         | 0.10087          | 0.09191           | 0.54406             | 0.07791             | 0.47152     | 0.27240             | 0 0 0 1       |
|                          | 4   | 0.25152             | 0.19490         | 0.17052          | 0.15869           | 0.54867             | 0.08278             | 0.46248     | 0.26479             | 0 0 0 1       |
|                          | 4   | 0.43074             | 0.29035         | 0.26803          | 0.25930           | 0.55996             | 0.15293             | 0.48710     | 0.31134             | 0 0 0 1       |

5. Simulation results analysis

Set parameters of CSA - BP neural network model, which is the number of nests  $n = 40$ ,  $P_a = 0.25$  and the maximum number of iterations  $N_{max} = 50$ . Topology structure of BP neural network is 8-8-4, hidden layer transfer function for the S-type tangent function is trainig, the output layer transfer function for the S-type logarithm function is logsig and training function selection is trainlm. The number of training is 1000, learning rate is 0.1 and training target is 0.0001.

Simulation results are shown in Fig. 16 and Fig. 17. BP neural network training iteration diagram shown in Fig. 18.

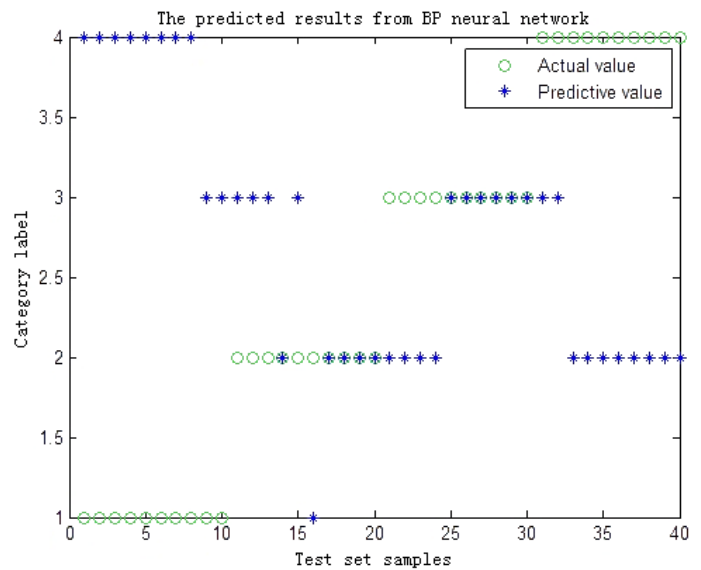


**Fig. 16.** BP neural network predicted results

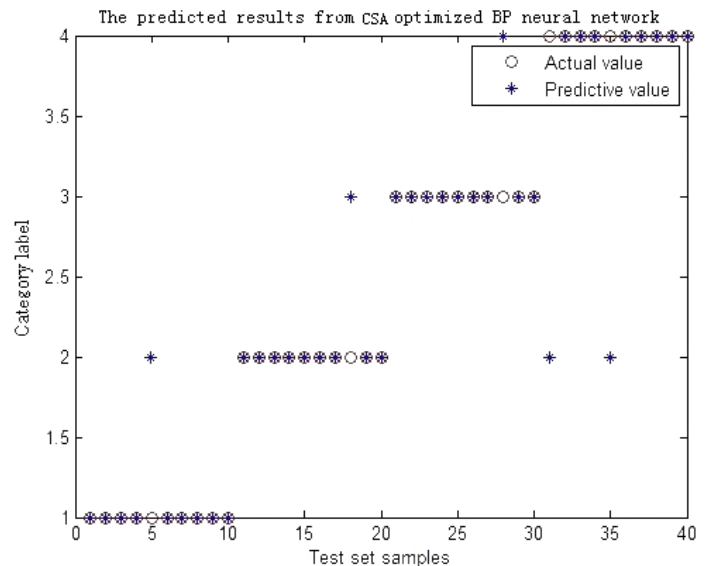


**Fig. 17.** CSA - BP neural network predicted results

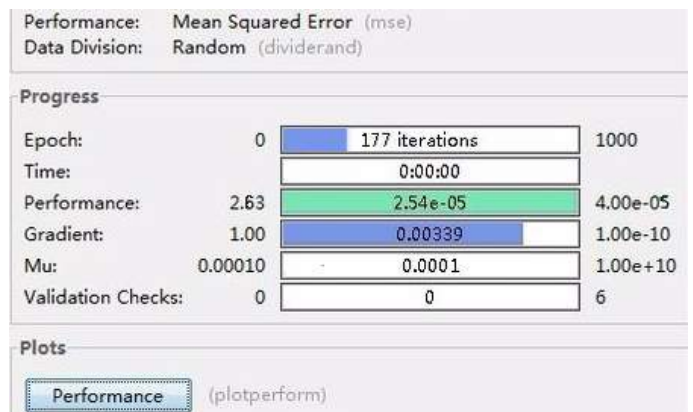


**Fig. 18.** BP neural network training iteration diagram

Using GA - BP neural network algorithm and PSO - BP neural network algorithm to judge the fault diagnosis of gearbox, the recognition results are shown in Fig.19. and Fig. 20.

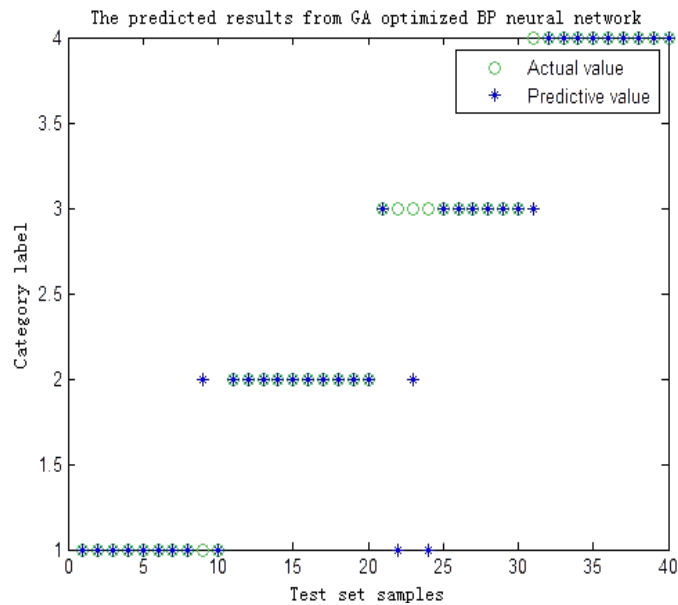


Fig. 19. GA - BP neural network predicted results

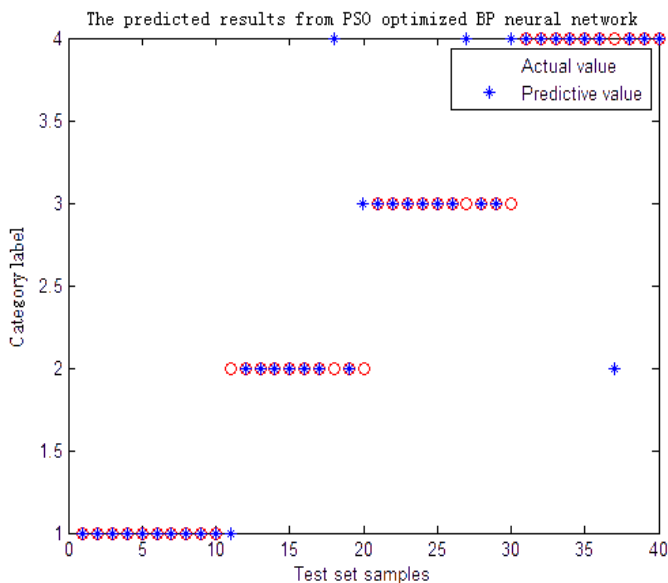


Fig.20. PSO - BP neural network predicted results

The above four kinds of recognition results are compared, as shown in Table.3.

Table. 3. BP, CSA - BP, GA - BP and PSO - BP recognition results of a comprehensive analysis

| No. | Algorithm | Identify the number of groups (40groups) | Accuracy (%) | Running time(s) |
|-----|-----------|--|--------------|-----------------|
| 1   | BP        | 11                                       | 22.5         | 23.52           |
| 2   | CSA -BP   | 35                                       | 87.5         | 104.59          |
| 3   | GA -BP    | 35                                       | 87.5         | 106.24          |
| 4   | PSO -BP   | 34                                       | 85           | 84.73           |

Through the analysis of Table 3, it can be seen that the accuracy of the recognition of the three algorithms has been greatly improved after BP neural network is optimized. Although the operating time has increased, but the increase is not much, which is 81.07s, 82.72s and 61.21s respectively. Comparing the recognition results, we can see that CSA - BP neural network algorithm and GA - BP neural network algorithm have the same correct rate, but CSA - BP neural network algorithm has relatively short running time. PSO - BP neural network algorithm running time is short, but the recognition accuracy rate is not as good as CSA - BP neural network algorithm. Comprehensive comparison of three optimization algorithms, we can draw a conclusion that CSA -BP neural network algorithm can get a good diagnosis in the gear fault as a new method.

V. CONCLUSION

Based on the four working conditions of the gearbox and BP neural network, this paper builds the algorithm model of CSA - BP neural network by using the advantages of CSA algorithm such as simple structure, less parameter setting and easy implementation. At the same time, combined with wavelet packet decomposition and reconstruction methods, the collected vibration signals are denoised, and then, carried on simulation analysis again. By comparing the result of analysis with GA - BP neural network and PSO - BP neural network algorithm, CSA - BP neural network algorithm model has good fault diagnosis performance. The diagnosis effect of this algorithm is accurate, which lays the foundation for timely and accurate identification of the fault type of the gearbox. It diagnosed the correct rate of 87.5 percent. Meanwhile, it can be known from the experiment that the training error is 0.0000254, which is less than the target value of 0.0001, which meets the forecasting requirements. Therefore, the intelligent algorithm is of great significance for reducing property damage and even personal injury caused by damage to equipment. At the same time, this method also indicates a new research direction for other mechanical fault diagnosis. What's more, it is very important to study the algorithm in the field of fault diagnosis.

REFERENCES

[1] X. S. Yang, S. Deb. "Cuckoo search via Lévy flights", *Nature & Biologic Inspired Computing*, IEEE Publications, USA, pp. 210-214, 2009.

- [2] H. Nie, B. Liu, and X. Y. Wei. "An improved cuckoo search algorithm for solving resource-constrained project scheduling problem", *Journal of Guilin University of Technology*, vol. 33, no.3, pp. 529–536, 2013.
- [3] L. Chen, W. Long. "An improved cuckoo search algorithm for solving optimization of engineering structures", *Application Research of Computers*, vol. 3, no.31, pp. 679–683, 2014.
- [4] C. M. Ye. "A cuckoo algorithm for solving the scheduling problem of permutation flow shop", *Shanghai University of Science and Technology*, vol. 35, no.1, pp. 17–20, 2013.
- [5] Q. Long, Y. Q. Liu, and Y. P. Yang. "Fault Diagnosis of Gearbox of Wind Turbine Based on Particle Swarm Optimization and BP Neural Network", *Journal of Solar Energy*, vol. 33, no.1, pp. 120–125, 2012.
- [6] L. W. Qi, G. Liang, and G. W. Tong. "Gearbox Fault Diagnosis Based on Optimum BP Neural Network with Drosophila Algorithm", *Power Grid and Clean Energy*, vol. 30, no.9, pp. 31–36, 2014.
- [7] Z. J. Zhao. "Traffic Prediction and Research Based on PSO - BP Neural Network", *Computer Applications and Software*, vol. 1, no.26, pp. 211–218, 2009.
- [8] J. L. Chen, Y. L. Fan, H. X. Ni, and W. Wu. "Time - Frequency Analysis and Endpoint Detection of Noisy Speech Based on Wavelet Packet Decomposition", *Data acquisition and processing*, vol. 29, no.2, pp. 293–297, 2014.
- [9] D. L. Lu, X. M. Guo. "Wavelet Packet Denoising Algorithm of Heart Sound Signal Based on Singular Spectrum Analysis", *Journal of Vibration and Shock*, vol. 32, no.18, pp. 63–69, 2013.
- [10] X. H. Fan, Z. J. Wang. "Evaluation and selection of characteristic parameters of mechanical system condition monitoring", *Journal of Armored Force Engineering*, vol. 3, no.23, pp. 25–28, 2009.

**Lijun Wang** was born on May. 16, 1971. She received the PhD degree in Signal and Information Processing from PLA Information Engineering University of China. Currently, she is a researcher (professor) at North China University of Water Resources and Electric Power, China. Her major research interests include signal processing, fault diagnosis and intelligent control.

**Shengfei Ji** was born on Feb. 6, 1990. He received Bachelor degree in Henan University of Engineering, Zhengzhou, China, in 2015. Now he studies at North China University of Water Resources and Electric Power. His current research interests include Signal processing, fault diagnosis and intelligent control.

**Nanyang Ji** was born on Aug.21,1993.He received Bachelor degree in Shangqiu Institute of Technology , Shangqiu, China, in 2017. Now he studies at North China University of Water Resources and Electric Power. His current research interests include Signal processing, fault diagnosis and intelligent control.